N O A A

FINAL REPORT

"A LASER PROBE FOR DETERMINING PHYSICAL OCEAN PARAMETERS"

By

J.G. Hirschberg, P.I., J.D. Byrne and A.W. Wouters

prepared for

U.S. Department of Commerce

NATIONAL OCEANIC and ATMOSPHERIC ADMINISTRATION

NOAA Grant No. 04-78-B01-5
10/1/1979 to 9/30/82

Laboratory for Optics and Astrophysics
of the
Department of Physics
University of Miami
Coral Gables, FL

C. Work Accomplished:

1. Field trial.

A preliminary field experiment was performed at the Florida Power and Light Company dock on Government Cut, Miami Beach, Florida. The site is on the north side of the channel 1.4 miles west of the ocean end of the jetty. At this point, the cut is about 500 yards wide and the main channel, dredged to a depth of about 30 feet, is 400 feet wide. At the dock itself, the depth was measured to be 26 1/2 feet at high water. Considerable tidal flow exists here and currents of 1 -3 knots were usual except for short periods at the stand of the tides. The water was never really clear, and was rather dirty much of the time with moving bits of weed, plankton and other material. We concluded that if it was possible to make observations under these conditions it would provide an excellent test of the method.

Oceanographic parameters measured:

1) Turbidity was measured by the time-honored Secchi method. A white sphere 25 cm in diameter was lowered into the sea and the depth measured when it disappeared from view. Secchi depths at the site ranged from 6 to 12 feet. This is to be compared to over 90 feet which we measured in water offshore in the Gulf Stream.

Temperature was measured using a thermistor and Wheatstone bridge which had been calibrated in the laboratory against a standard thermometer. These measurements are probably accurate to 1/5 degree Celsius.

The salinity was not measured directly, and we assumed an average value of 35 parts per thousand. In future work, when equipment is available to warrant it, the salinity will be measured by standard methods.

A surplus Navy argon-ion R.C.A. laser was used at 4880 Å or 20492 cm^{-1}.

The laser beam was projected nearly vertically downward into the water and the returning light passed through an interference filter and a Fabry-Perot interferometer and was measured with a photomultiplier. Good fringes of the Brillouin peaks were obtained[4], when the interferometer was swept with Freon 12.

The pressure-scanned Fabry-Perot produced fringes as the Freon pressure dropped from about 10 to 0 psig. Scans were usually of about 10 minute duration before the pressure was reset.

The tracings were then averaged together to eliminate the effects of random electronic noise and short-term fluctuations of turbidity. Values of the amplitude of the fringes at uniform separations on the tracing were tabulated. The position of the center of the laser line of each order was calculated. The uniform separation of the data points was adjusted to fit the actual fringe spacing. A lagrangian four - point interpolation was used to fit a curve to the data. The values of this curve at fifty evenly spaced points in each order were added together over 17 traces. The averaged data is plotted in Fig. 2. The quality of the results is clearly seen since the theoretical points from a convolution of an interferometer instrumental function with deduced positions of the Brillouin peaks agree with the averaged experimental points to within $\pm$ 0.5 percent. This corresponds to a temperature scatter of $\pm$ 1.5°C. It was recognized that these results were preliminary and served only to show the feasibility of this method; accuracies ultimately available will be considerably better, as will be shown below.

The turbidity of seawater was determined by taking the ratio of the integral over wavelength of the central peak fringe to that of the Brillouin peak. A graphical integration of the average of three orders was made to provide turbidity information. This ratio was about 300 to 1 for the water in Government Cut. For pure water in the laboratory the ratio was 1.7 to 1, and for tap water the ratio was 14.7 to 1.

2. Improvements for Higher Accuracy

It was decided that greater accuracy was necessary, in the next phase to at least half a degree Celsius.

New apparatus was therefore constructed, consisting of coaxial projection and collection beams at sea. At the same time, we have built a more sophisticated optical system combining a Michelson interferometer with two Fabry-Perot interferometers.

A new laser was purchased, both much more powerful and more stable than the surplus Navy Laser formerly used. It is a coherent CR-6 6 watt argon-ion laser with a model 423 etalon for stabilization.

The Michelson was added to reduce the effect of the Tyndall undeviated light, and effectively make it possible to work in much more turbid water. It also serves to separate the Tyndall and Brillouin components, which facilitates turbidity measurement. The Michelson interferometer, when

collimated, has a transmission function $I = I_0 \cos^2(2x/\lambda)$, as shown in Figure 3. Since energy is not lost in the system (assuming lossless mirrors and beam splitters, which is a good approximation since multiple dielectrics are used) the returning beam is the complement of the transmitted beam, as shown.

The Michelson is used to separate the Brillouin components from the unshifted Rayleigh-Tyndall component, taking advantage of the zeros of the $(\cos)^2$ function to minimise the unshifted component in Beam A (Figure 3) and vice versa for Beam B. The situation for Beam A is shown in Figure 4. The maxima in the $(\cos)^2$ function are so broad that they have almost no effect on the Brillouin peaks if properly adjusted, as shown. The back-reflected Beam B, containing the unshifted Rayleigh-Tyndall scattering is reflected by Beam-Splitter S_1 (Figure 5) which consists of an ordinary piece of plate glass (reflection coefficient about 8%) into a photomultiplier, P_1. The output of P_1 is proportional to the turbidity of the water. This measurement is not wasteful of the fainter, Brillouin light, since only about 8% is used.

Beam A, containing the Brillouin scattering peaks, is sent to a 50-50 beam splitter, S_4 in Figure 5, and directed to the two Fabry-Perot interferometers, C and D. These are equiped with spacers fixing their free spectral ranges, S, as shown in Figure 4 with Fabry-Perot C slightly smaller and Fabry-Perot D slightly larger. The spacers are 0.824 and 1.006 cm respectively, yielding free spectral ranges, S, of 0.607 and 0.497 cm^{-1}. The result for Fabry-Perot C, for example, is shown in Figure 7. The measurement is made at the pattern center. If the wavelength shift increases, for example, the intensity at the center rises, and vice versa. For Fabry-Perot D, the inverse obtains. This occurs since the two free spectral ranges just bracket the Brillouin shift for average conditions in the sea.

If now the ratio of the output of photomultipliers P_2 and P_3 is calculated, it will be proportional to the position of the Brillouin components. The temperature is in turn proportional to the wavelength separation of the Brillouin components, as explained in the section on Theory, above. The resulting behavior of the outputs P_2/P_3 is plotted against temperature in Figure 6.

3. Computer Calculations

It is of interest to ascertain the most advantageous arrangement of parameters to measure the Brillouin temperature. Accordingly, we plotted the effect of changes in the finesse, f, of the Fabry-Perot interferometer on the central part of the Fabry-Perot trace of the Brillouin spectrum. In each case the ratio of the central (undeviated) intensity to the Brillouin intensity is 25. Finesses are a:3, b:5, c:7, and d:9. Note the advantage of greater finesse in that the change in central intensity between each curve (a change of about 5°C) is greater for greater finesse. This is plotted in Figure 8, where 5°C increments are shown.

Another parameter of interest is the height of the central (undeviated) peak. In Figure 9 are shown a number of similar plots of the Fabry-Perot pattern showing the two Brillouin peaks first unresolved and then well resolved as they separate. Effective temperature change between each curve is about 5 degrees C. The sets of curves show the effect of the comparitive strength of the central (undeviated) peak. The ratios are: a 10 to 1, b 50 to 1, c 150 to 1 and d 400 to 1. In each case the undeviated line is the stronger. Note that the effect of the Tyndall peak on the measurement is minimal, even when the central peak is 400 times stronger than the Brillouin lines. The finesse, is 8 for all the curves, a value which is reasonable for our present interferometers. These data indicate that measurements will be meaningful even to very turbid conditions at finesse = 8, or even 6.

4. Experimental results

Figure 10 shows a typical result. The temperature of a scattering cell was varied and the Brillouin shifts measured. By averaging over 10 minute intervals the temperatures are seen to fall on the straight line to better than 0.2°C. Since temperature-controlled standards can be used, it is reasonable to expect the same accuracy in the field.

D. Conclusion

We have proposed a new method for measuring sound velocity, temperature and turbidity at depth in the sea. Its advantages are speed and accuracy. Our original measurements in sea water from a stationary platform (a dock) showed that the method had promise, but indicated the need for greater accuracy. Our latest laboratory measurements give a strong indication that

accuracies to 1/10 degree celsius are obtainable. We conclude that with better interferometers, (e.g. Piezo electric, stabilized to 1/200 λ) which are now commercially available, combined with more sophisticated data-handling gear, we can extend these same accurate measurements to the field. If this is true, a wealth of phenomena in the sea concerning the behavior of internal waves, sound propagation, and biological environment will become available for accurate study.

E. References

1. Hirschberg, J., A. Wouters, F. Cooke, K. Simon and J. Byrne
   Laser application to measure vertical sea temperature and turbidity, NASA Report NASA CR-139184, January, 1975.

2. Hirschberg, J., A. Wouters and J. Byrne
   Laser measure of salinity, temperature and turbidity in depth, Remote Sensing Energy Related Studies, ed. N. veziroglu, Wiley & Sons, New York. (1975)

3. Hirschberg, J.G.
   The use of Brillouin and Raman scattering to measure temperature and salinity below the water surface. Waste Heat Management and Utilization Conference, Miami Beach FL, May 11, 1977.

4. Hirschberg, J.G., A.W. Wouters and J.D. Byrne
   "Ocean Parameters Using the Brillouin Effect".
   Symposium: Ocean Remote Sensing Using Lasers, NOAA, Patricia Bay, B.C. 1978. Progeedings.

5. Hirschberg, J.G. and J.D. Byrne
   "Brillouin Spectrum Measurement of Ocean Parameters."
   Optics News 7, 3 p. 81 (1981).

F. Acknowledgements

Besides the NOAA Grant, this work was also supported by:

United States Navy: Loan of Laser

NASA: U.S. National Aeronautics and Space Administration Grants NAS10-8600 and NAS10-8795, "Laser Application of Measure Vertical Sea Temperature as Remote Sensor," 1976-1978

and Grant NASA NAGW-258 "Laser Brillouin Probe for Measuring Sea Parameters from a Submerged Vehicle" 1981-1983

Florida Power and Light Company, Miami FL: use of dock at Government Cut Plant, Miami Beach FL 1977-1978.

The University of Miami Friends of Physics: Gift to help purchase new laser.

The Principal Investigator wishes to express his appreciation for the above.

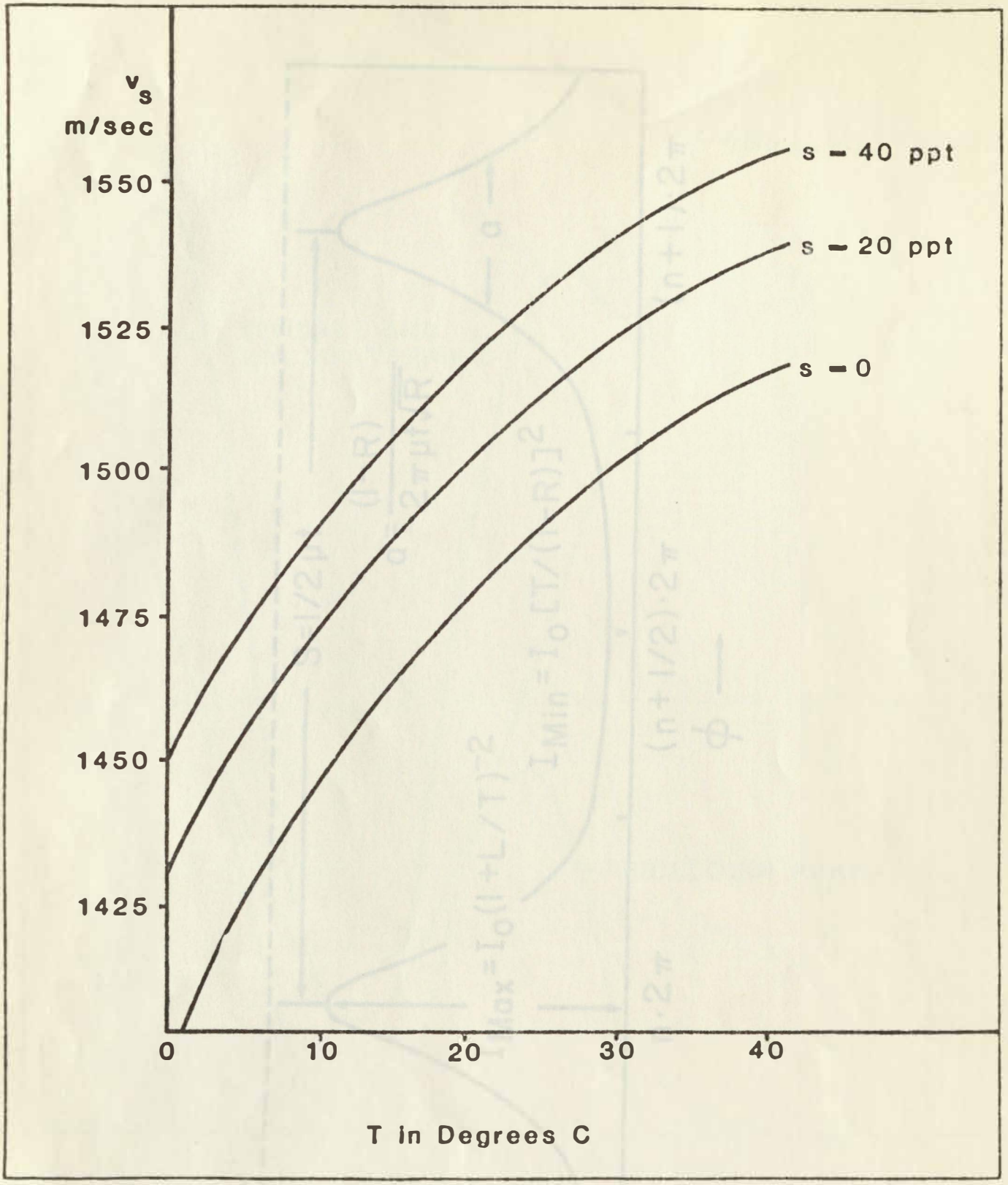

Figure 1A. Sound velocity of v_s plotted against temperature T for various values of salinity (redrawn from R. J. Urick, Principles of Underwater Sound for Engineers).

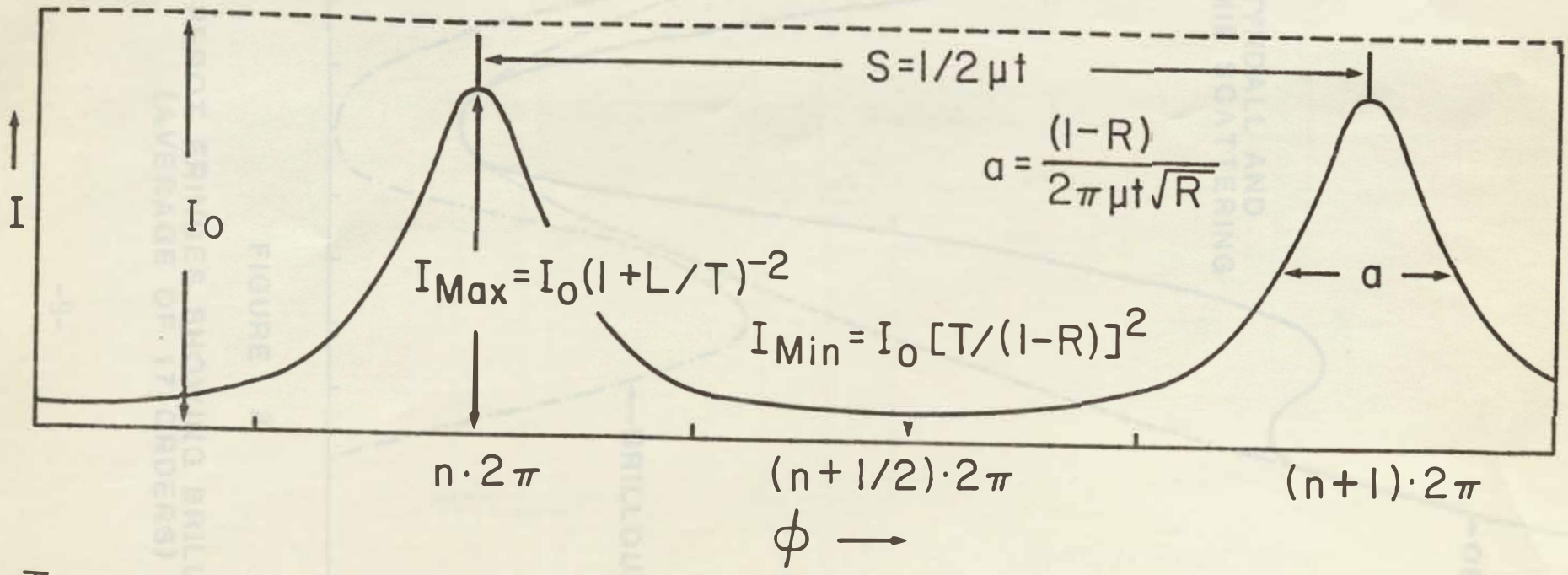
S=1/2μt
$a = \frac{(1-R)}{2\pi\mu t\sqrt{R}}$
I
I_o
$I_{Max} = I_o(1+L/T)^{-2}$
$I_{Min} = I_o[T/(1-R)]^2$
a
$n \cdot 2\pi$
$(n+1/2)\cdot 2\pi$
$(n+1)\cdot 2\pi$
ϕ ⟶

FIGURE 1B

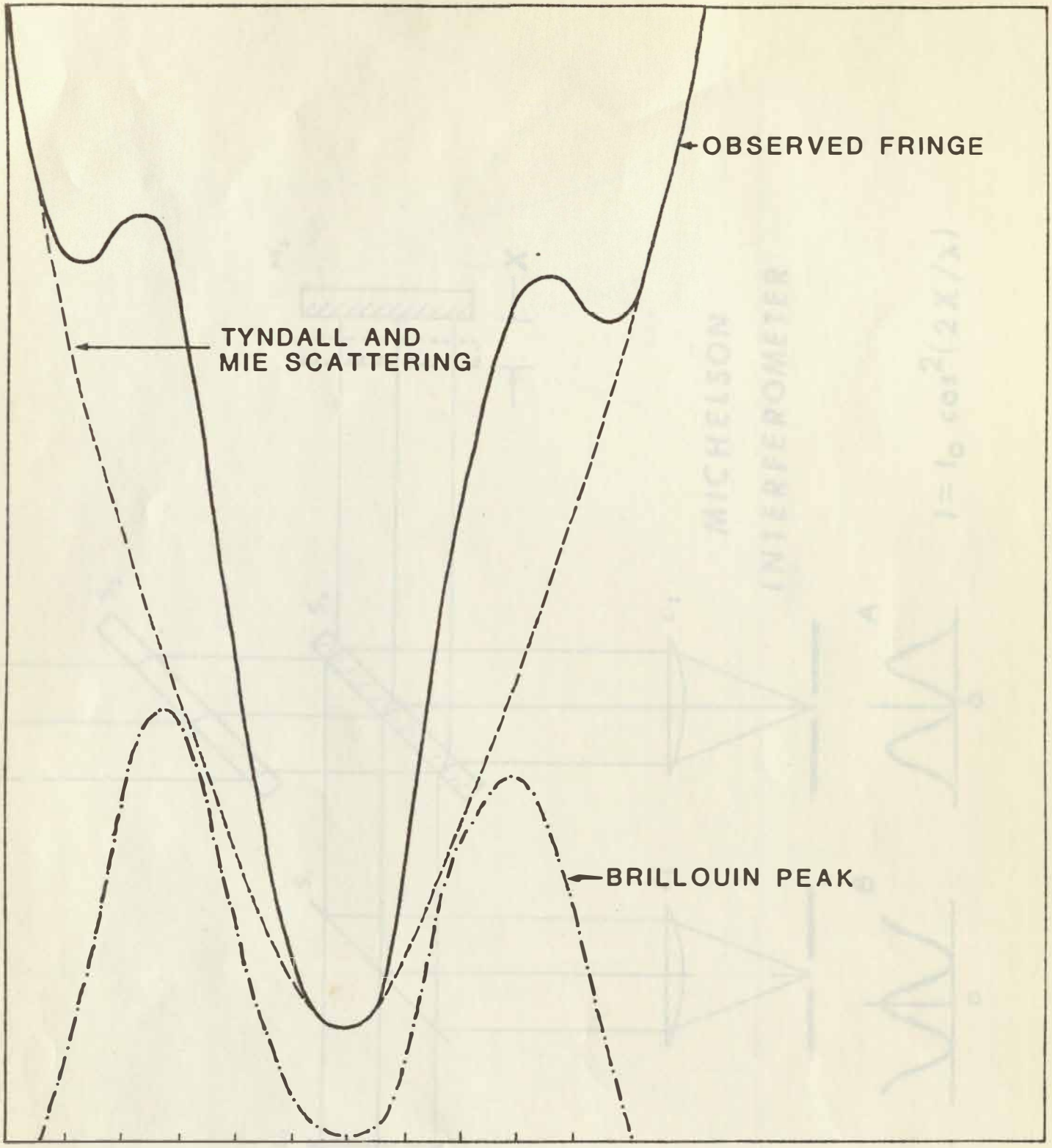

FIGURE 2

FABRY - PEROT FRINGES SHOWING BRILLOUIN EFFECT
(AVERAGE OF 17 ORDERS)

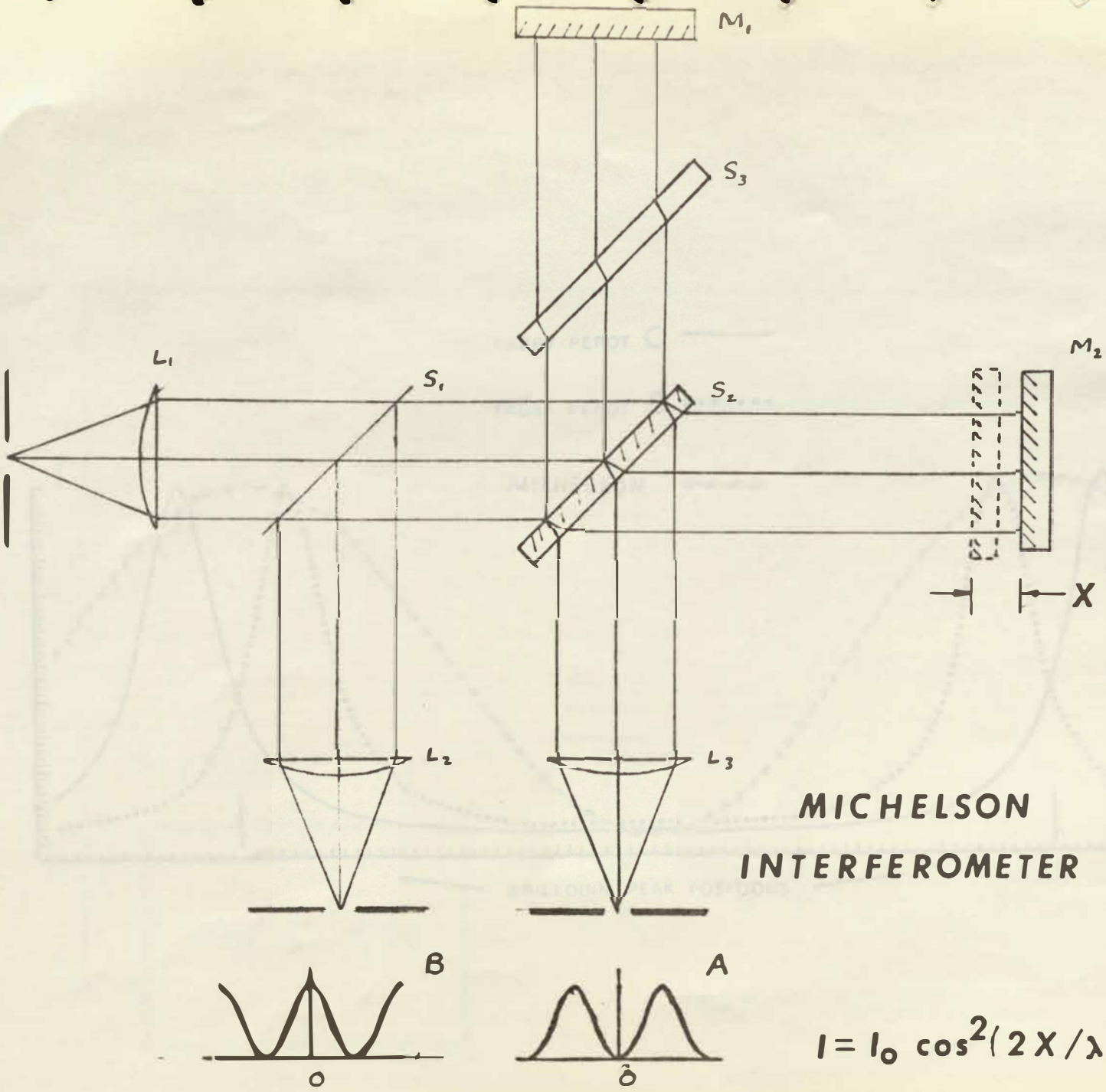

MICHELSON INTERFEROMETER

$$I = I_0 \cos^2(2X/\lambda)$$

FIGURE 3

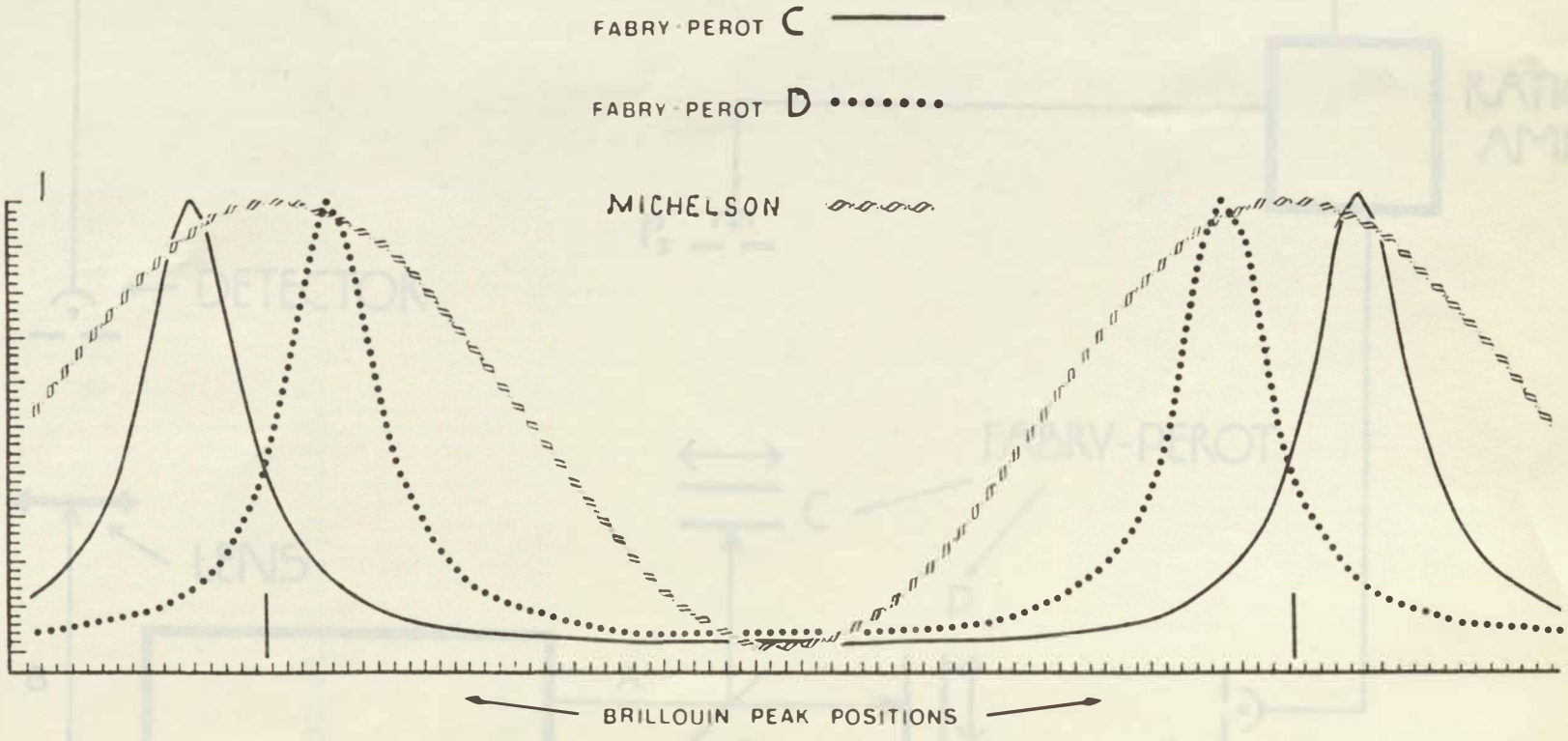
FABRY-PEROT C
FABRY-PEROT D
MICHELSON
BRILLOUIN PEAK POSITIONS

FIGURE 4

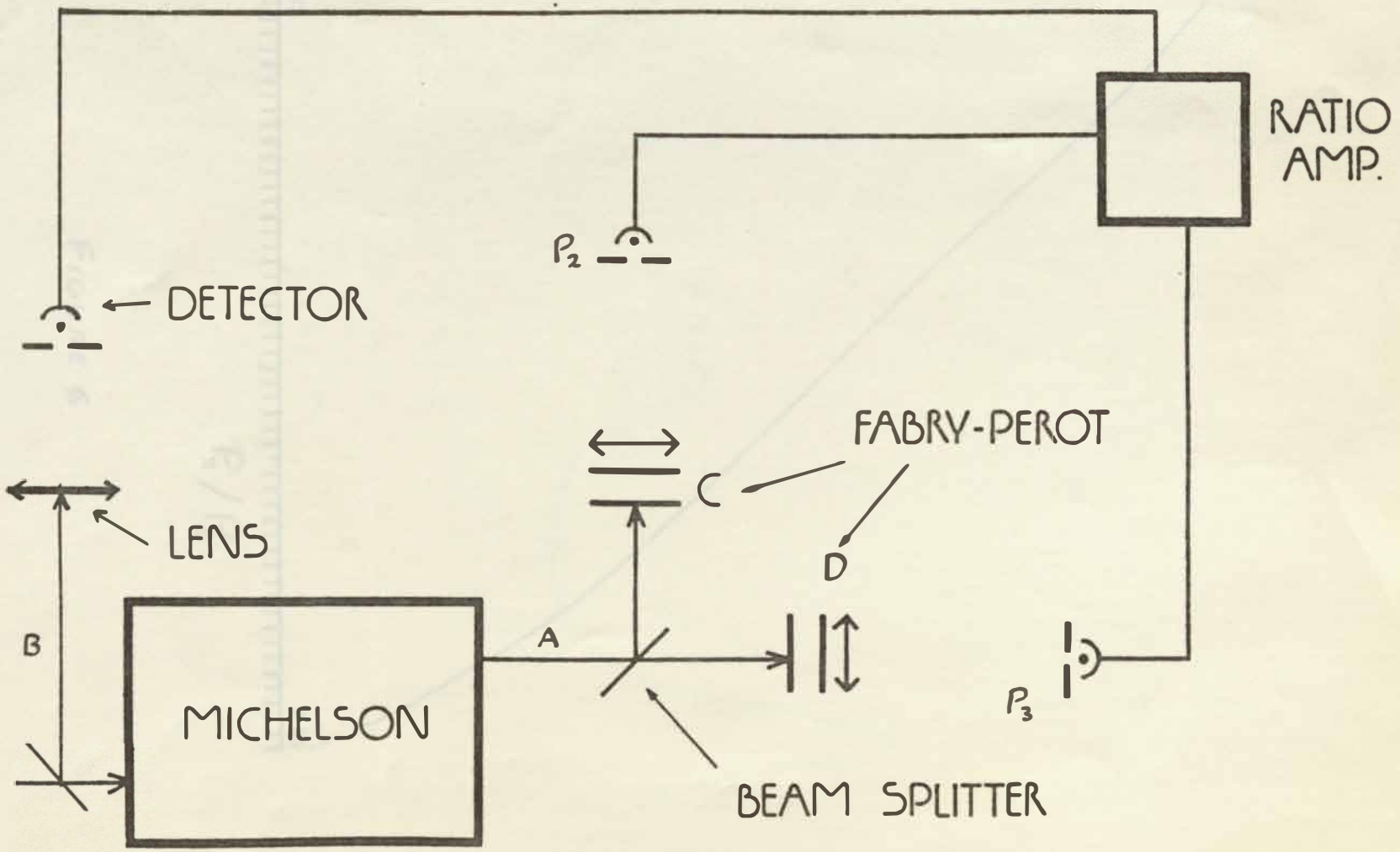
RATIO
AMP.
P_2
DETECTOR
FABRY-PEROT
C
D
LENS
B
A
MICHELSON
P_3
BEAM SPLITTER

FIGURE 5

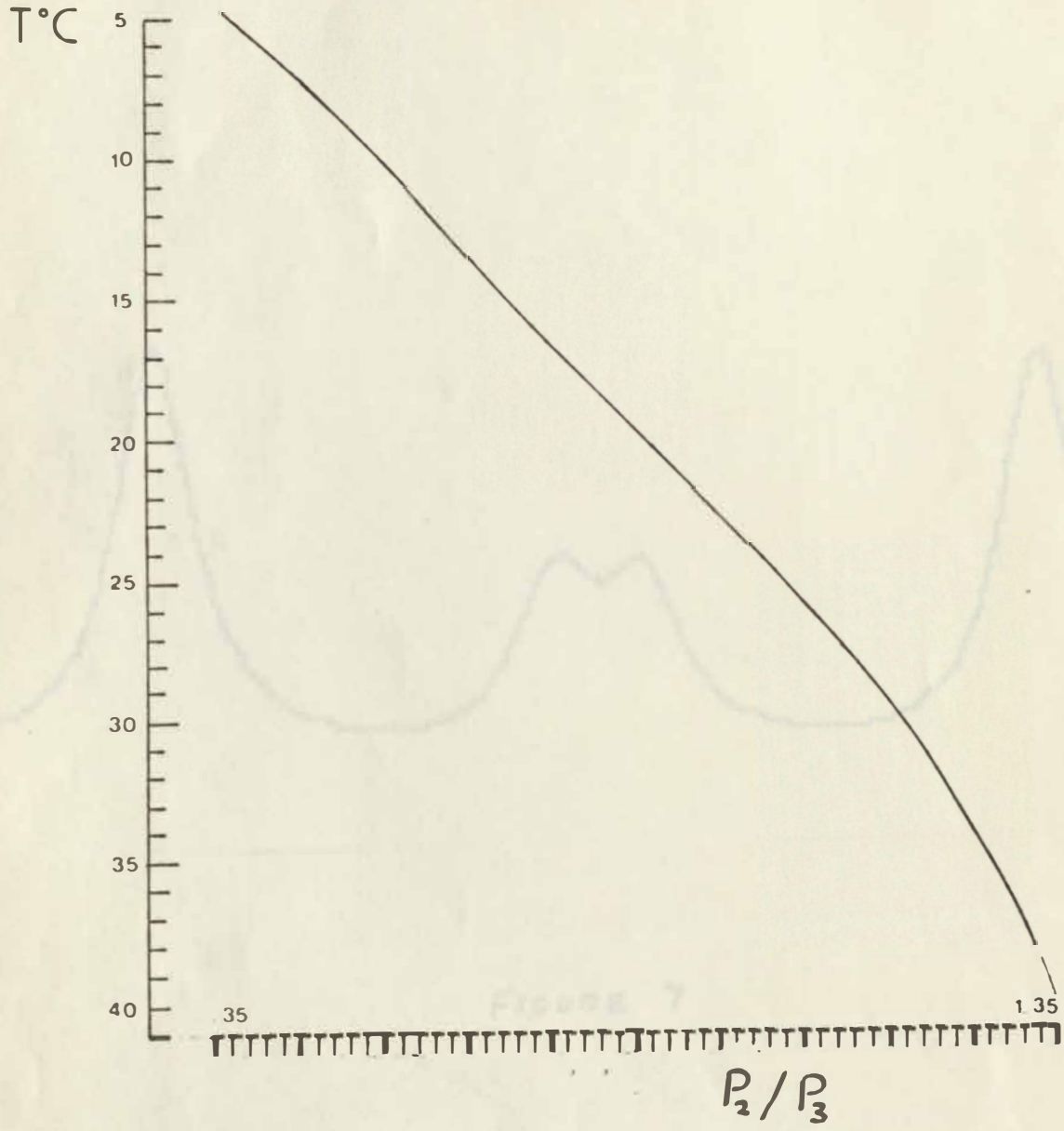

FIGURE 6

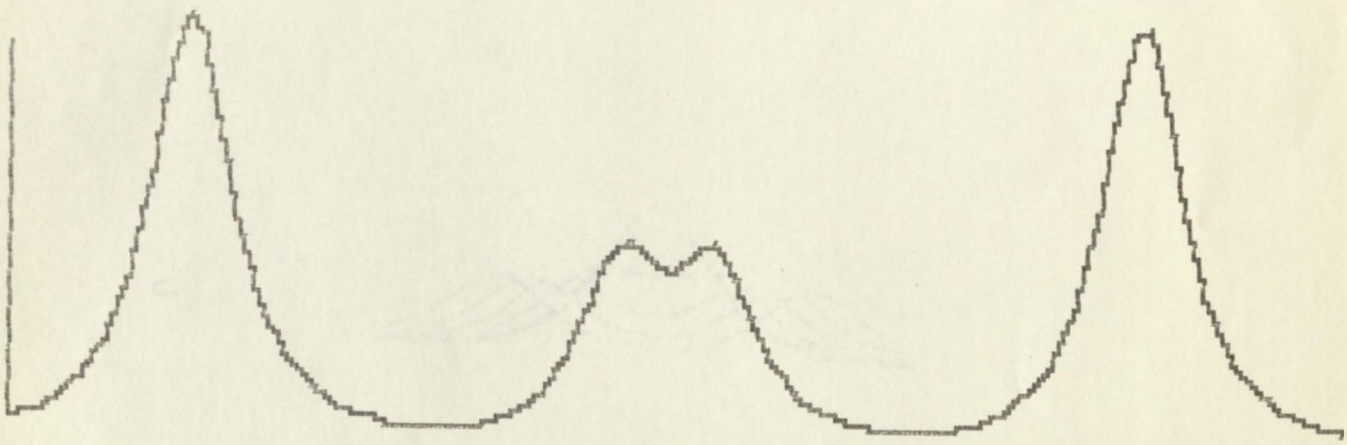

FIGURE 7

a.

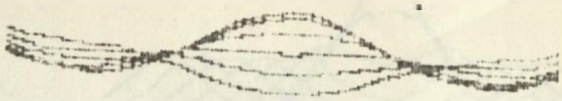

b.

c.

d.

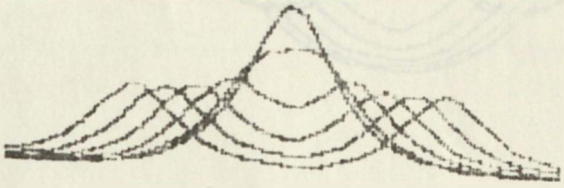

Figure 8

a.

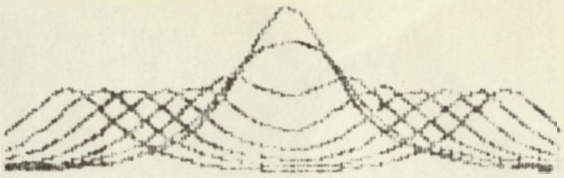

b.

c.

d.

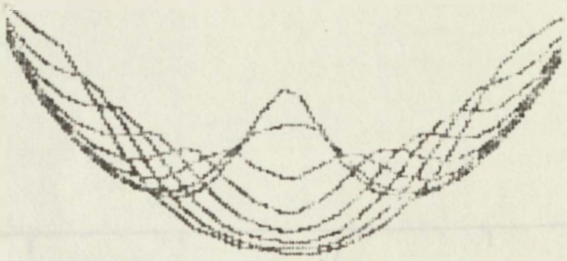

Figure 9

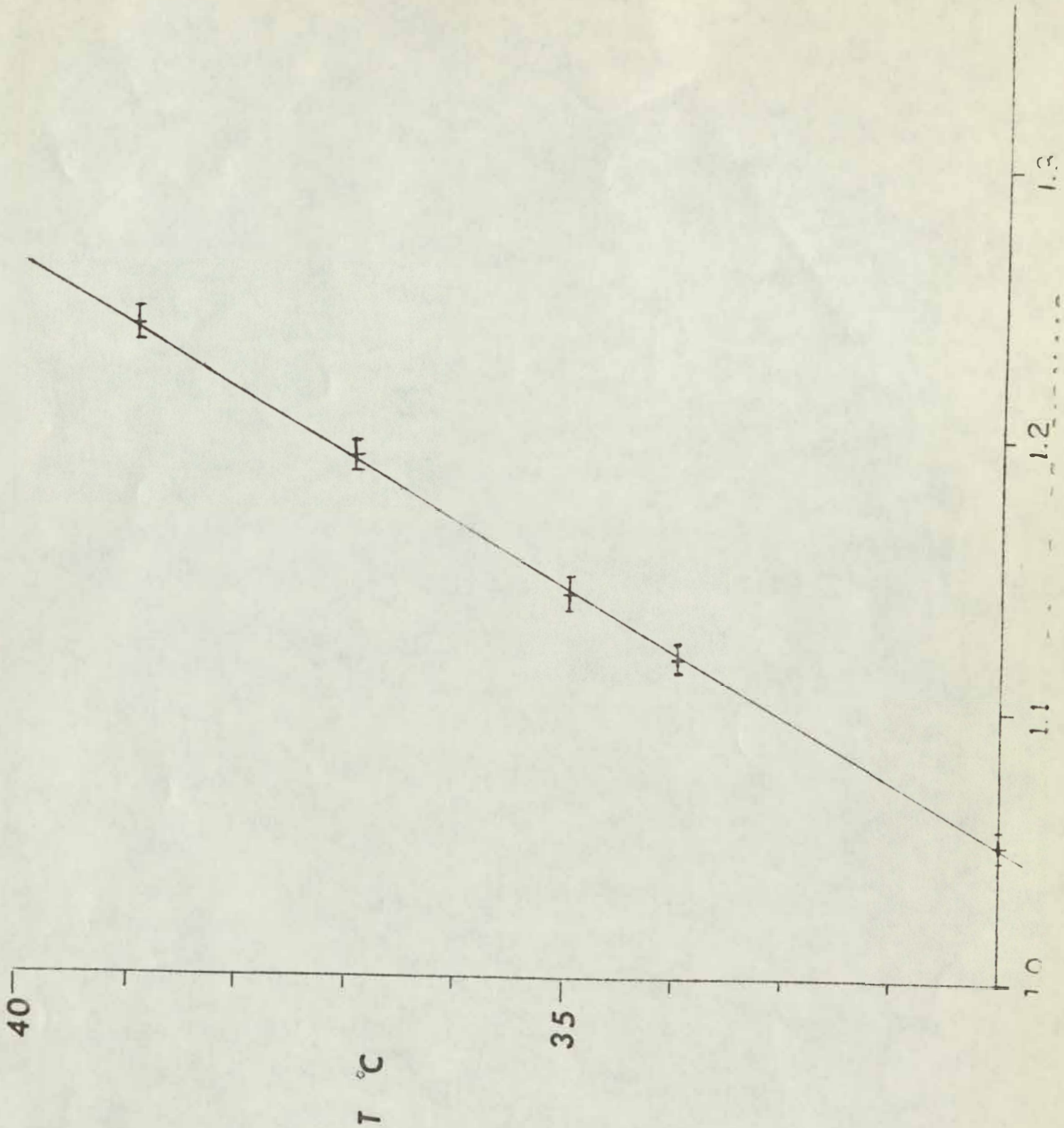

FIGURE 10